A Theoretical Model for Indirect Dissociative Electron Attachment

Iwona Anusiewicz,[†,‡,§] Monika Sobczyk,[†,‡] Joanna Berdys-Kochanska,[†,‡] Piotr Skurski,[†,‡] and Jack Simons*[,†]

Chemistry Department and Henry Eyring Center for Theoretical Chemistry, University of Utah, Salt Lake City, Utah 84112, and Department of Chemistry, University of Gdansk, 80-952 Gdansk, Poland

Received: July 12, 2004; In Final Form: November 4, 2004

In this paper, we describe a computational model that allows us to avoid having to perform a very large number of tedious calculations on electronically metastable anions when studying indirect DEA processes. By indirect, we mean that the electron attaches to an orbital in one region of the molecule but a bond is subsequently broken in another region. For such events, one must describe the coupling between two diabatic anion states, corresponding to the occupation of orbitals in the two regions of the molecule, to achieve a correct description. We introduce a simple 2 × 2 matrix model as well as physically reasonable and computationally efficient approximations to the diabatic states in regions where they are metastable. We show this model to be highly effective when applied to several indirect DEA processes that we studied earlier with brute-force methods. The main advantage of using this model is that one can avoid having to carry out a large number of calculations on metastable anion states; only one or two such calculations are required.

I. Introduction

A. Direct Dissociative Electron Attachment. In a direct dissociative electron attachment (DEA) process, a free electron having kinetic energy E strikes a molecule A−B in which the fragments A and B are chemically bonded and enters directly into an antibonding orbital (e.g., a S−S σ^* orbital in MeS−SMe), after which the nascent A−B$^-$ anion can undergo either electron autodetachment or A−B bond cleavage to form A + B$^-$. Such a process is illustrated in Figure 1, where the bound A−B and repulsive (A−B)$^-$ potential energy surfaces are also shown.

Let us consider an example of such a direct DEA event. It has been determined[1] that electrons having kinetic energies near 1 eV can enter into the S−S σ^* orbital of dimethyl disulfide (MeS−SMe) and cause S−S bond rupture to form the MeS radical and the MeS$^-$ anion. In such processes, the dissociation yields depend on the competition between the rate of motion on the repulsive (A−B)$^-$ anion surface (the black curve in Figure 1) and the rate of electron autodetachment (represented by the green arrow in Figure 1). The shorter the autodetachment lifetime, the smaller the DEA yield; the steeper the repulsive curve, the prompter the dissociation, and thus, the higher the DEA yield.

B. Indirect Dissociative Electron Attachment. Indirect DEA processes are different because they involve attaching an electron to a vacant orbital in one region of the molecule while breaking a bond in another region. An example of such a process is shown in Figure 2, in which the olefin π^* orbital is where the electron attaches but the C−Cl σ bond is where the dissociation occurs.[2]

In such indirect DEA processes, there are two anion states that must be considered: one with the excess electron in the olefin π^* orbital and the other with the electron in the C−Cl σ^* orbital. The appropriate potential energy curves for these two diabatic anion states are shown qualitatively in Figure 3 as functions of the C−Cl bond length (because this is the bond that ultimately is cleaved).

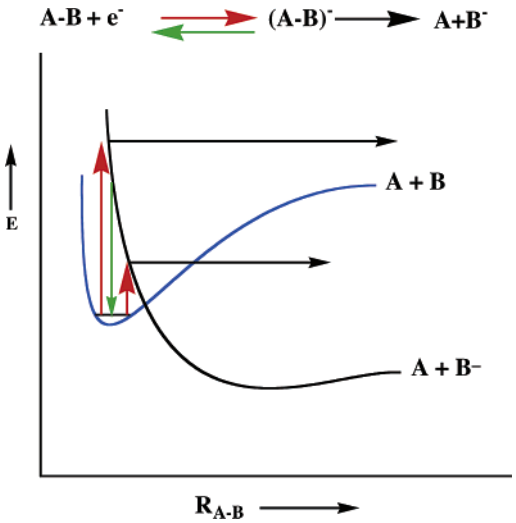

Figure 1. Depiction of electron capture (red arrows), autodetachment (green arrow), and dissociation (black arrows) arising when an A−B molecule is struck by an electron and forms an A radical and a B$^-$ anion via direct DEA.

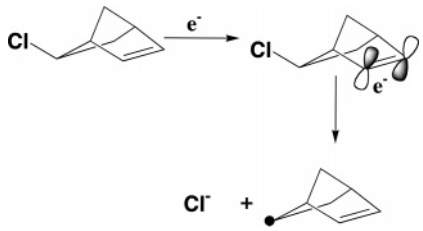

Figure 2. Illustration of indirect DEA in which an electron enters a π^* orbital and subsequently fragments the C−Cl σ bond to form the Cl$^-$ anion and a hydrocarbon radical.

Note that the π^* anion curve is drawn as nearly parallel to the neutral molecule's energy curve along the R_{C-Cl} coordinate

* Corresponding author. E-mail: simons@chemistry.utah.edu.
† University of Utah.
‡ University of Gdansk.
§ Holder of a Foundation for Polish Science (FNP) Award.

10.1021/jp046914f CCC: $30.25
Published on Web 12/30/2004

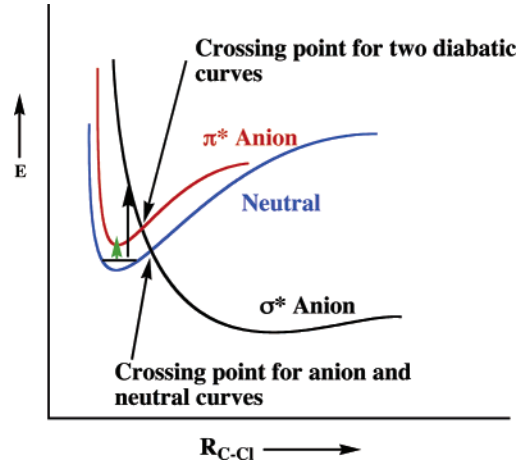

Figure 3. Illustrative plots of the neutral, σ^* anion, and π^* anion states (e.g., relating to the species shown in Figure 2) as functions of the C−Cl bond that ruptures.

(because placing an electron into the π^* orbital does not qualitatively alter the C−Cl σ bonding), whereas the σ^* anion curve is repulsive near the equilibrium C−Cl bond length as expected (because having the excess electron in the σ^* orbital ruptures this bond). The facts that the repulsive σ^* curve lies far below the neutral curve at large R and intersects the neutral curve not far above the neutral's minimum relate to the very large electron affinity of the Cl atom.

In the indirect DEA of the cyclic compound shown in Figure 2, an electron having kinetic energy E appropriate to enter the π^* orbital of the olefinic unit[3] attaches to this orbital (illustrated by the green arrow in Figure 3) to initially form the metastable π^*-shape resonance anion. This anion can subsequently undergo electron autodetachment (at a rate of ca. 10^{14} s^{-1}), or it can evolve, through coupling with the C−Cl σ^* resonance state, to break the C−Cl σ bond and form the Cl^- ion and the hydrocarbon radical. The coupling between the π^* and σ^* states occurs most strongly when the C−Cl bond is stretched to near the point where these two diabatic curves cross (see Figure 3). That is, the two diabatic states couple to produce a pair of adiabatic states; upon the lower-energy adiabatic surface, the reactive flux then evolves. Once on the repulsive σ^* component of this adiabatic curve, the molecule can dissociate to form the Cl^- and hydrocarbon radical products, but it can also undergo electron detachment (at a rate of ca. 10^{15} s^{-1}) until the σ^* anion's curve crosses below that of the neutral.

It should be noted that, at low electron energies, the σ^* anion state is not directly (i.e., vertically) accessible (black vertical arrow in Figure 3) because it vertically lies at significantly higher energies than does the π^* anion.[4] Moreover, only at very stretched bond lengths does the σ^* anion approach and intersect the neutral; therefore, unless the sample is very hot, it is highly improbable that the neutral's bond length will be so extended as to allow zero-energy electrons to attach directly near such a neutral−anion curve crossing. Of course, as noted earlier, both the π^* and σ^* anions' energies are Heisenberg broadened by significant amounts,[3] so the above observations need to be softened to take these widths into consideration. In particular, the large width of the σ^* state can allow it to attach electrons of considerably lower energy (even down to zero energy) than one would expect on the basis of the above analysis, although with continuously decreasing probability as one moves farther from the central energy of the resonance state.

It should also be noted that the outward motion of the nascent anion formed vertically in the indirect DEA process will be impeded by a barrier on the adiabatic surface near where the π^* and σ^* diabatic curves intersect and couple most strongly. Therefore, unlike the direct DEA case, in which the nascent anion surface is purely repulsive, it is not competition between autodetachment and prompt/direct fragmentation that governs the yield of dissociation. For indirect DEA, the competition also involves accessing the barrier on the anion's adiabatic surface; in fact, it is primarily the rate at which this barrier is accessed that, in competition with autodetachment, governs the dissociation yield.

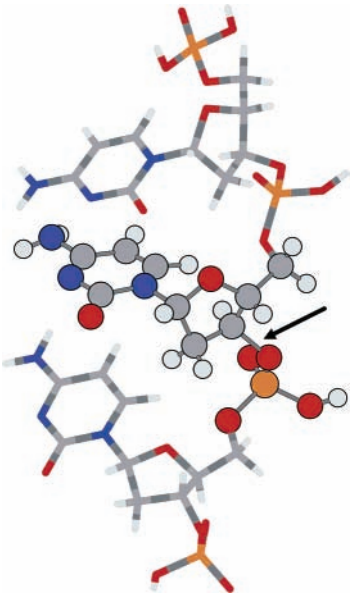

Figure 4. CCC codon used in one of our earlier studies.[9] The central cytosine−sugar−phosphate unit is shown in ball-and-stick format while the π-stacked neighboring units are shown in stick format.

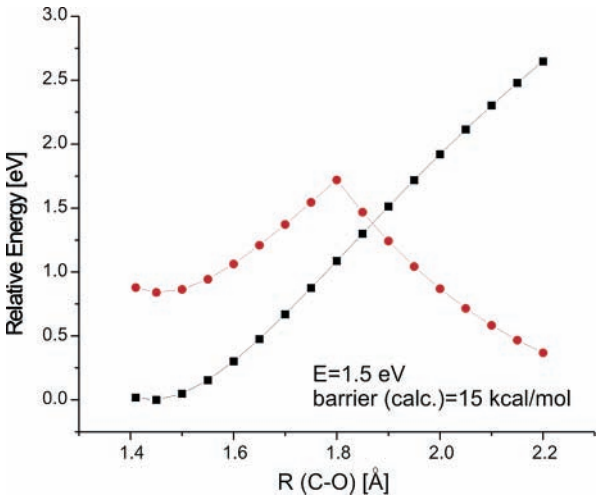

Figure 5. Plots of the neutral (squares) and adiabatic anion (circles) electronic energies as functions of the sugar−phosphate C−O bond length for a fragment of DNA consisting of three cytosine−deoxyribose−phosphate units[9] arranged in a π-stacked fashion as shown in Figure 4. In this example, an excess electron with a kinetic energy of 1.5 eV (within the Heisenberg width of a π^* resonance) attaches. The barrier on the anion's adiabatic surface lies 15 kcal mol^{-1} above the anion's local-minimum energy (i.e., near 1.45 Å).

II. Overview of Our Earlier Work Involving Indirect DEA in Biological Molecules

Recently, we have devoted a great deal of effort to computing, using ab initio electronic structure methods, the neutral and

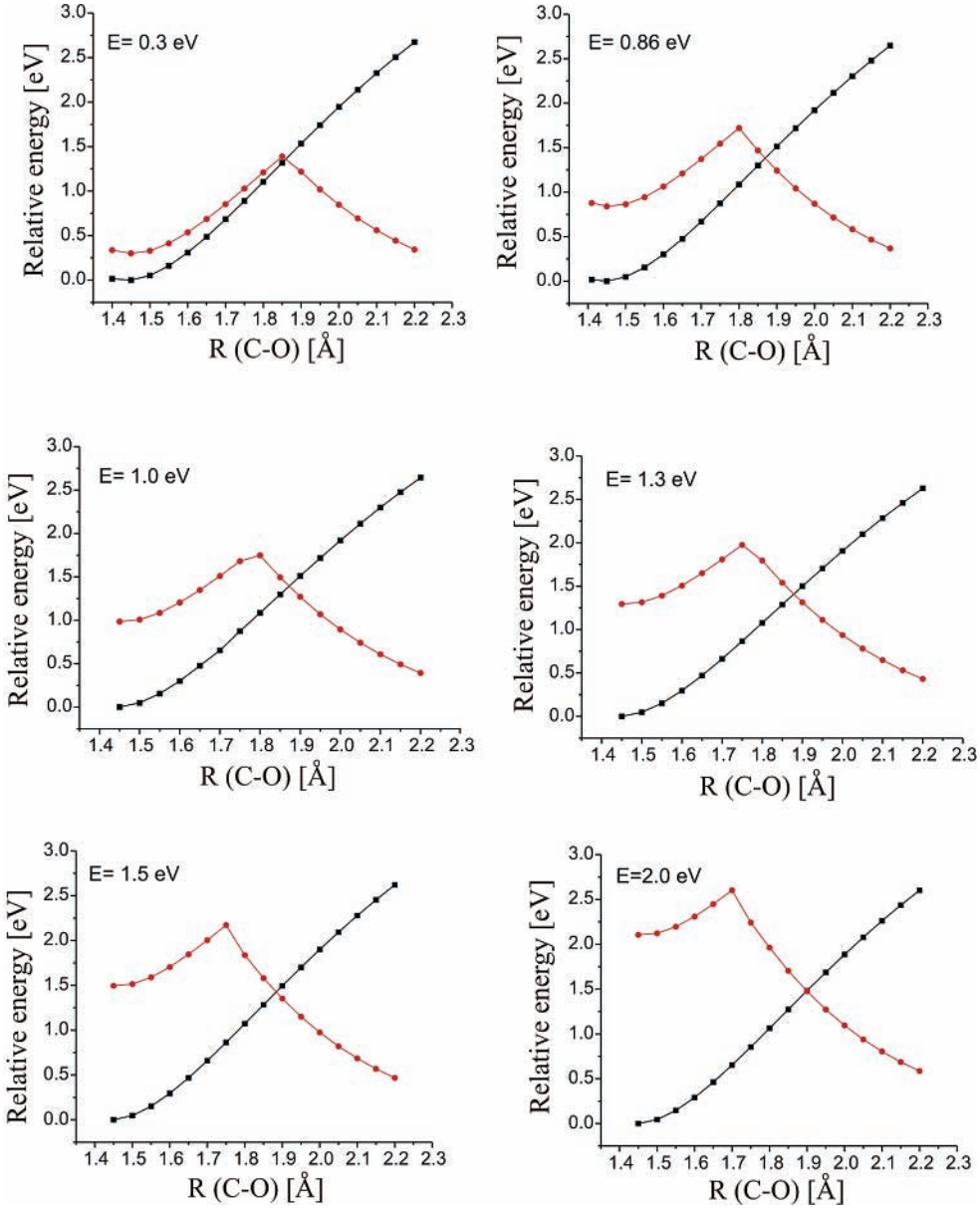

Figure 6. Plots of the neutral (squares) and adiabatic anion (circles) electronic energies as functions of the sugar−phosphate C−O bond length for the CCC codon fragment shown in Figure 4 for a variety of electron kinetic energies lying within the Heisenberg width of the π^* resonance.

lowest adiabatic anion curves for species consisting of fragments of DNA involving a base connected to a deoxyribose and then to a phosphate group.[5−8] This work relates to our interest in the mechanisms by which low-energy electrons can cause structural damage in DNA. In such cases, it is believed that a low-energy (i.e., 0.2−2 eV) electron attaches to a π^* orbital of one of DNA's bases, but that a sugar−phosphate C−O σ bond is subsequently ruptured. As such, these are indirect DEA situations as we discussed earlier. An example of the kind of data we produced for the CCC codon depicted in Figure 4 is shown in Figure 5.

In Figure 6, we illustrate how the anion and neutral surfaces for this same CCC codon vary[9] as one alters the kinetic energy E of the attached electron from 0.3 to 2.0 eV to cover the majority of the Heisenberg width of the π^* resonance state studied.

As discussed in our earlier works,[5−9] the adiabatic anion state in such cases consists of a dominantly valence π^* state (with the excess electron occupying a π^* orbital of the cytosine fragment, as we determined by inspection) for $R < 1.75$ Å and a dominantly σ^* state for larger R values (with the electron occupying a sugar−phosphate C−O σ^* orbital, which we also determined by inspection). These data therefore offer an example of the indirect DEA process discussed above in which the incident electron attaches (vertically near $R = 1.45$ Å) to form a π^* anion that evolves, as the C−O bond length stretches to near 1.75 Å, into a σ^* anion that then fragments to produce the very stable phosphate anion and a sugar-based carbon radical. The barrier on the anion's adiabatic surface plays a central role in determining the rate at which C−O bond cleavage occurs. It is clear from Figure 6 that this barrier changes as the incident electron's kinetic energy E changes; as a result, the rate of C−O bond cleavage varies with E.

In addition to the CCC codon illustrated in Figure 4, we examined single cytosine−sugar−phosphate units[5,6] as well as individual thymine−sugar−phosphate units[8] to determine their rates of C−O bond cleavage at various electron energies. We carried out such studies both in the absence of any stabilizing solvation environment and with solvation strengths (using the PCM model[10]) ranging up to a dielectric constant of $\epsilon = 78$.

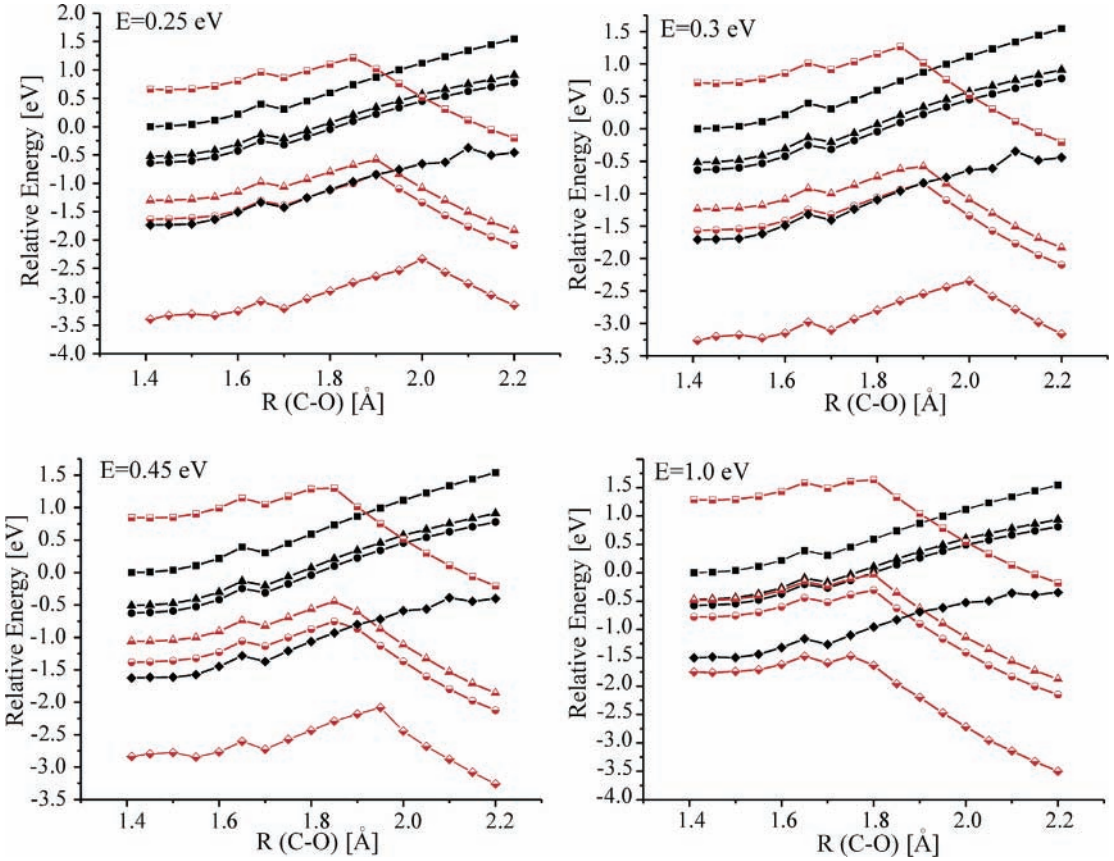

Figure 7. Energies of thymine sugar−phosphate neutral fragment ($\epsilon = 1.0$, solid square; $\epsilon = 4.9$, solid triangle; $\epsilon = 10.4$, solid circle; $\epsilon = 78$, solid diamond) and of adiabatic anion ($\epsilon = 1.0$, half-filled square; $\epsilon = 4.9$, half-filled triangle; $\epsilon = 10.4$, half-filled circle; $\epsilon = 78$, half filled diamond) fragment at various electron energies E and various solvation dielectric constants ϵ.

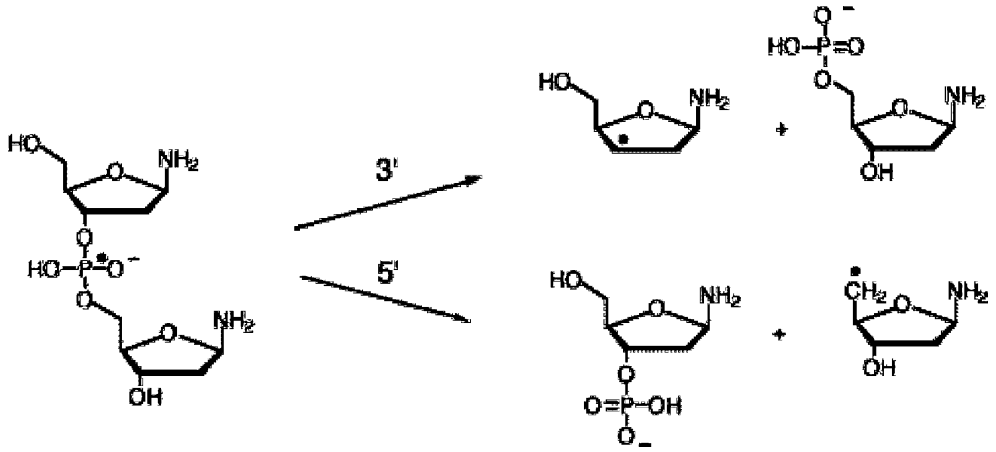

Figure 8. Phosphate radical anion center formed by attaching an electron to the π^* orbital of a P═O bond and subsequent 3′ and 5′ fragmentation of phosphate−sugar O−C bonds.

The potential energy curves we generated for the thymine−sugar−phosphate case[8] are shown in Figure 7 as illustrative examples.

Finally, also as part of our DNA-damage research, we studied[7] processes in which a free electron having energy E strikes the π bond of a phosphate unit, (RO)(R′O)(HO)P═O, that is bonded in 3′ and 5′ manners to two sugar units (labeled R and R′). Such model compounds were selected because this kind of structural motif occurs in DNA. When the phosphate group's π bond is struck, a $-P^{\bullet}-O^{-}$ radical anion center is formed, as shown in Figure 8, and subsequently, an O−C σ bond connecting the phosphate to one of the sugar groups is broken.

In our study of this system, we calculated both the diabatic π^* and σ^* energies, as well as the neutral energy curves, as functions of the phosphate−sugar O−C bond (3′ or 5′) shown in Figure 9.

Of course, we were also able to compute the lowest adiabatic anion surface for this case, but we do not show this in Figure 9.

There are two very important observations we need to make concerning the data shown in Figures 6, 7, and 9, which are characteristic of all of the results that we have obtained to date:

(1) The σ^* diabatic curves (alternatively, the large-R σ^* component of the adiabatic curves) all display the characteristic

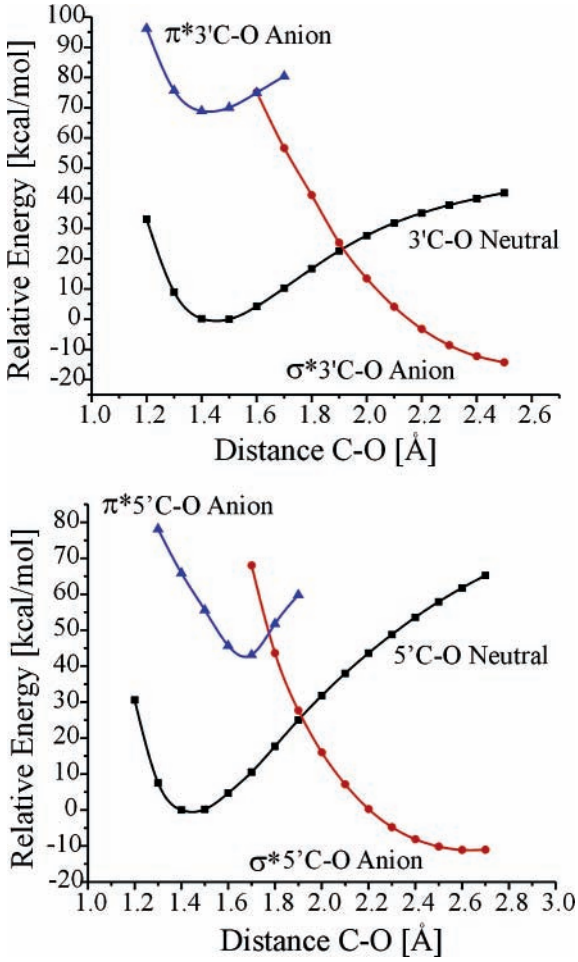

Figure 9. Diabatic anion and neutral energies of the sugar−phosphate−sugar unit shown in Figure 8 as functions of the C−O bond that is stretched to effect the 3′ or 5′ cleavage.

purely repulsive form[11] and have large-R asymptotes whose energies (relative to the neutral) reflect the electron detachment energy (>4 eV) of the phosphate anion formed when σ bond rupture occurs.

(2) The π^* diabatic curves (alternatively, the small-R π^* component of the adiabatic curves) are all nearly parallel to the neutral's curve but shifted upward by an amount equal to the π^* state's resonance energy at the equilibrium geometry of the neutral. This does not mean that structural changes do not occur when an electron enters the π^* orbital. They certainly do, and they were considered in our work on the species discussed here. However, the changes occur primarily within the framework of the π bonding of the cytosine, thymine, or P═O units.

These two observations pertain to our CCC codon data, our thymine−sugar−phosphate data, our cytosine−sugar−phosphate data, and our sugar−phosphate−sugar data and remain valid regardless of whether we include solvation effects (e.g., see Figure 7).

The fact that the π^* anion state parallels the neutral curve along the C−O coordinate is, of course, not surprising in the CCC, cytosine, and thymine cases because placing an electron into a base π^* orbital causes no significant alteration to the bonding within the rather distant C−O σ bond. In the phosphate−sugar−phosphate example (Figure 9), the π^* anion and neutral curves are not as parallel as in the other examples, which is not surprising given the much greater proximity of the phosphate π^* orbital to the C−O σ bond that ruptures. Nevertheless, the two characteristics noted above (repulsive σ^* state and π^* state parallel to the neutral) are central to the model that we now introduce; later, we examine how well the model does even for the phosphate attachment case where we expect it not to be as reliable for the reason just stated.

III. The Model for Indirect DEA

A. Why Do We Need a Model? If we have been able to calculate the neutral and diabatic π^* and σ^* (and adiabatic) curves for the species discussed above, why do we need to introduce any model? The primary reason is to eliminate much of the computational expense involved in performing such calculations. In particular, for values of the bond length R where the π^* and/or σ^* diabatic states lie above the energy of the corresponding neutral, these anion states are not bound but are electronically metastable. As such, their energies cannot be evaluated by straightforward application of quantum chemistry methods. It is well-known that calculations on such states will undergo "variational collapse"[12] as the atomic orbital basis set is expanded (e.g., by adding more and more diffuse functions) and will yield an energy equal to that of the neutral molecule plus a free electron infinitely distant and with essentially zero kinetic energy. That is, the excess electron will not remain within the π^* or σ^* orbital but, to achieve a lower total energy, will "escape" to large distances and attain very low kinetic energy.

To overcome such difficulties, we have had to make use of so-called stabilization methods[13] that allow us to properly evaluate the electronic energies of such metastable states. However, such calculations are extremely computationally intensive,[14] so it would be of considerable benefit to us (and hopefully to others) if we could avoid some of these calculations. It is largely for this reason that we think the model put forth here offers great promise.

B. What Is the Model? The following elements constitute the computational model we put forth in this work:

(1) We admit that we need to compute the energy of the neutral species (i.e., the electronic energy as a function of the length R of the bond being considered for breakage with all other geometrical degrees of freedom relaxed to minimize the energy).

(2) We also accept that we need to compute the σ^* diabatic curve of the anion at larger R values where this anion is electronically stable. Neither these calculations nor the calculation of the neutral curve require any of the special "tricks" of the stabilization method.

(3) We posit that the energy curve for the π^* diabatic state of the anion (at least in a substantial neighborhood of the neutral's equilibrium bond length) can be approximated by shifting the neutral's curve upward in energy by the kinetic energy of the incident electron E. Of course, we must know that this energy lies within the Heisenberg width of the π^* resonance state, so either the position (i.e., central energy) and width of this state must be known or we must compute them. In the works discussed here, we assume that we have computed the position using stabilization-type methods discussed in our earlier papers, and we assumed the widths to be those typical of π^* resonances (i.e., ca. 0.5 eV). We denote the diabatic π^* energy curve[4] at bond length R by $E_{\pi^*}(R)$.

(4) We posit that the σ^* curve of the anion can be extrapolated (e.g., using an exponential form[15] appropriate to such a repulsive potential) inward to smaller R values where this σ^* diabatic state of the anion is metastable. We denote this diabatic σ^* curve by $E_{\sigma^*}(R)$.

(5) We next postulate that the σ^* and π^* diabatic states couple via a scalar (i.e., R-independent)[16] matrix element

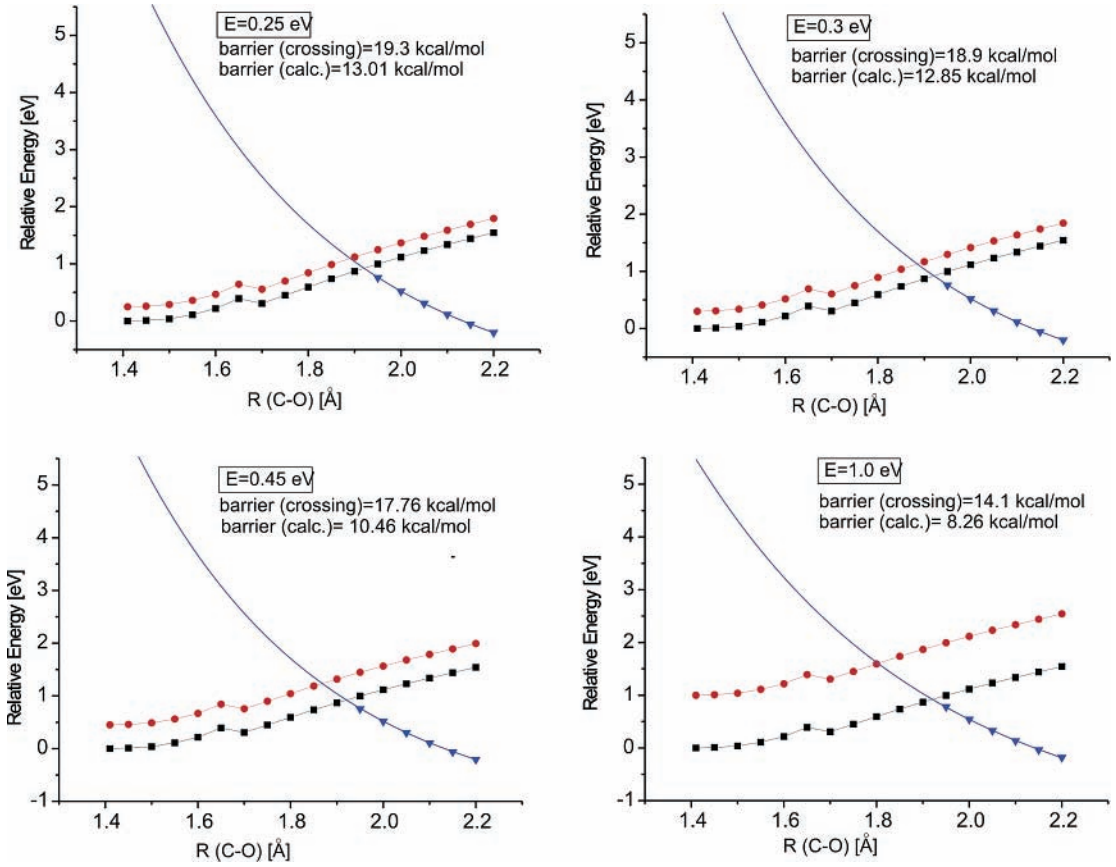

Figure 10. Neutral (black), approximate diabatic π^* anion (red), and diabatic σ^* anion (blue; see text for details) curves for thymine−sugar−phosphate system as functions of the sugar−phosphate C−O bond length with all other geometrical degrees of freedom relaxed.

$\langle\sigma^*|H|\pi^*\rangle = V$ and that the lower (and upper) adiabatic states that arise from such coupling can be obtained as eigenvalues of a 2 × 2 Hamiltonian matrix of the form

$$\begin{bmatrix} E_{\pi^*}(R) & V \\ V & E_{\sigma^*}(R) \end{bmatrix}.$$

(6) The two adiabatic energies can be obtained at any R value by solving the quadratic secular equation associated with this matrix

$$E_{\pm} = \frac{1}{2}[E_{\pi^*}(R) + E_{\sigma^*}(R)] \pm \frac{1}{2}\sqrt{[E_{\pi^*}(R) - E_{\sigma^*}(R)]^2 + 4V^2}$$

(7) To obtain the magnitude of the coupling matrix element $|V|$, we must carry out a single stabilization calculation[13] on the lower adiabatic metastable state of the anion at that value of R where the diabatic π^* and σ^* curves intersect.[17] According to the above quadratic equation, the result we obtain for E_- at this R value lies an amount $|V|$ below the energies of the π^* and σ^* diabatic states. Thus, we take $|V| = E_{\sigma^*} - E_-$.

(8) Knowing $|V|$, we can then evaluate the lower (and upper) adiabatic energies at any R value by using

$$E_{\pm} = \frac{1}{2}[E_{\pi^*}(R) + E_{\sigma^*}(R)] \pm \frac{1}{2}\sqrt{[E_{\pi^*}(R) - E_{\sigma^*}(R)]^2 + 4V^2}$$

at that value of R. This allows us to generate the full upper and lower adiabatic surfaces.

(9) If one is interested in the strength of the through-bond electron transfer that allows the excess electron to migrate from the initial π^* orbital to the σ^* orbital, this is given by $|V|$. In turn, the rate of the electron transfer is given as $2|V|/\hbar$.

C. Examples of How the Model Works. Let us now examine several applications of this model and compare its predictions with the fully ab initio adiabatic curves that we earlier obtained at great computational expense. In Figure 10, we show (1) the neutral energy curve appropriate to the thymine sugar−phosphate model system studied in ref 8, (2) the corresponding σ^* diabatic curve computed for R values where this state is electronically stable and extrapolated to smaller R using the exponential form discussed earlier, and (3) a diabatic π^* curve approximated by the neutral curve shifted to higher energy by an amount E equal to the kinetic energy of the attached electron (all of these energies lie within the Heisenberg width of the π^* state).

For comparison, the thymine−sugar−phosphate fully ab initio neutral and lowest adiabatic anion curves appear above in Figure 7.

The energies listed in Figure 10 as barrier (crossing) and barrier (calc) are, respectively, the energy gap from the minimum in the π^* curve to where the π^* curve intersects the extrapolated σ^* curve and the fully ab initio energy gap from the minimum on the lowest adiabatic anion curve and its barrier. The barrier (crossing) data are not the final estimates of the model presented in this paper, but are simply approximations based on where the two diabatic curves intersect. Our final estimates, obtained from our 2 × 2 model, are shown in Figure 11 for the thymine−sugar−phosphate case.

Using the above data for $E_{\sigma^*}(R)$ and $E_{\pi^*}(R)$ and carrying out a single stabilization calculation of the lowest[18] adiabatic energy E_- at a value of R at or near the crossing of the two diabatic curves, we were able to compute $|V|$ and to thus evaluate both

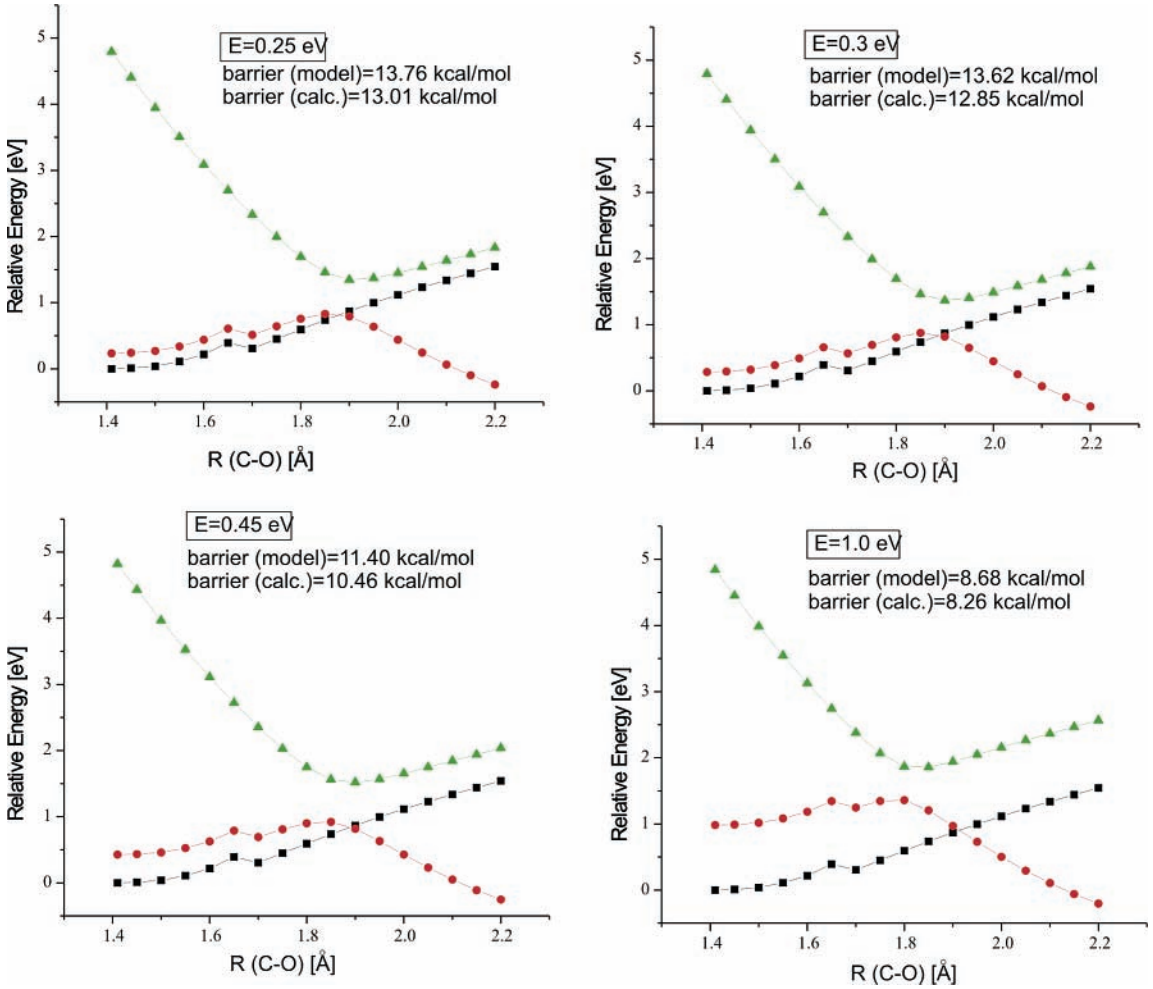

Figure 11. Neutral (black), lowest (red), and upper (green) adiabatic energies resulting from our model for the thymine−sugar−phosphate system.

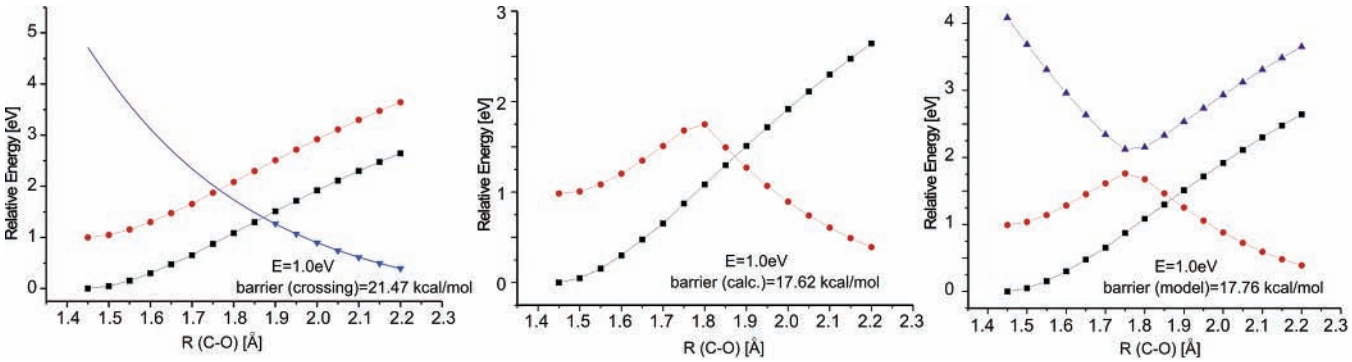

Figure 12. Energy curves for the CCC codon obtained as approximate diabatic curves of our model (top), from full ab initio calculations (center), and as a result of our 2 × 2 matrix model (bottom).

adiabatic surfaces for the full range of R values using the quadratic expression given earlier. In Figure 11 we show the two adiabatic anion surfaces that result for each of the four energies E.

Listed in Figure 11 are the barriers along the lowest adiabatic anion surface (i.e., from that curve's minimum near 1.4 Å to its barrier near 1.8 Å) for each of the four electron energies E as well as the corresponding barriers obtained in our earlier fully ab initio calculations whose curves appear in Figure 7. Clearly, there is remarkable agreement between the barriers resulting from our 2 × 2 matrix model and the fully ab initio barriers even though the model required us to perform only a single difficult stabilization calculation on the metastable lowest anion adiabatic state. We also note that the barrier heights obtained by locating the intersections of the σ^* and π^* diabatic states (see Figure 10) are not very accurate estimates of the ab initio barriers. It is important to include the σ^*/π^* coupling, as reflected in the energy lowering by $|V|$, to obtain accurate barriers as in Figure 11. We also note that the differences between the barrier (model) data in Figure 11 and those obtained from the σ^*/π^* intersection points as in Figure 10 (i.e., barrier (crossing)) are precisely the $|V|$ values of our model. These $|V|$ values range from 5 to 6 kcal mol^{-1} for the thymine−sugar−phosphate system and thus correspond to through-bond electron-transfer rates of 10^{13} s^{-1}.

Now consider another example, that of the CCC codon to which a 1.0 eV electron is attached whose data is summarized in Figure 12.

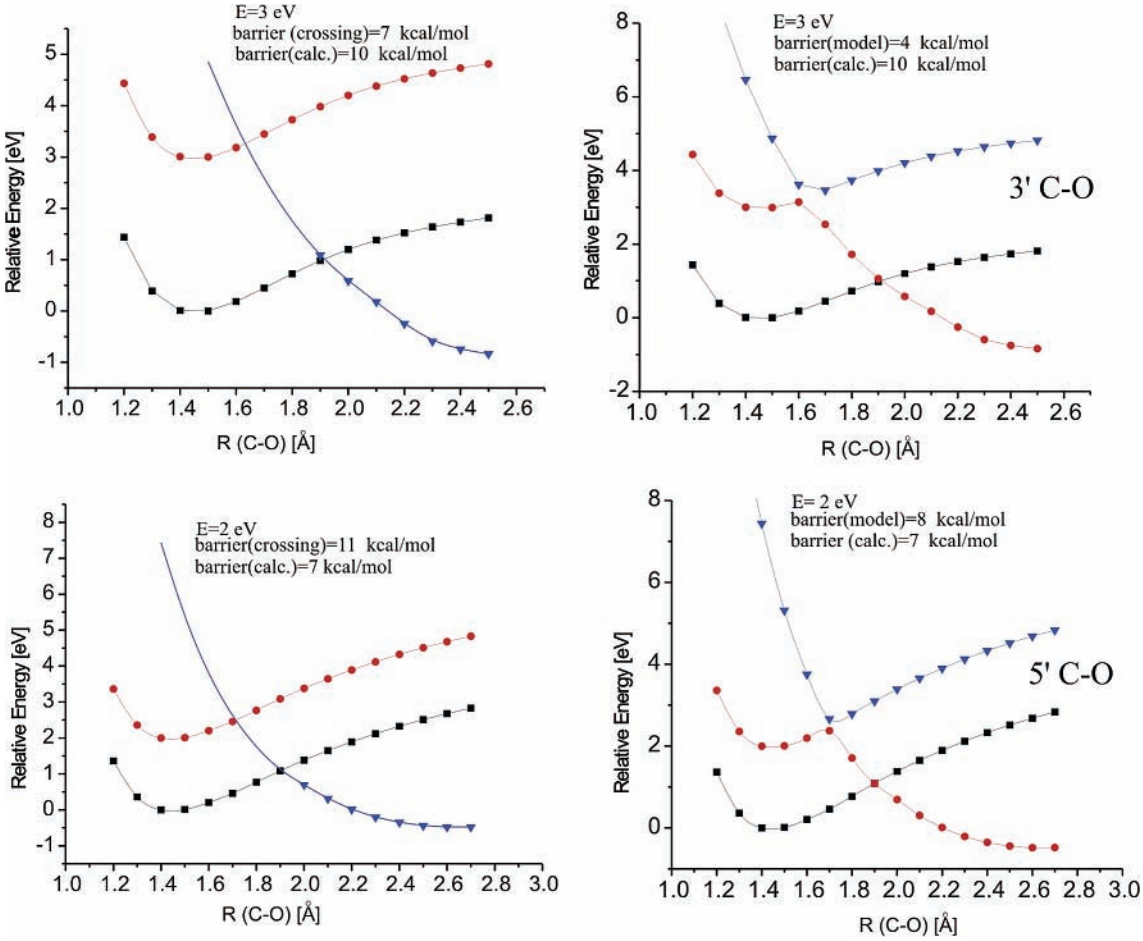

Figure 13. Results for the sugar−phosphate−sugar compound of Figure 8 for $E = 2.0$ and 3.0 eV. On the left are approximate (model) diabatic curves for the neutral, σ^* and π^* anion. On the right are the adiabatic curves resulting from the 2×2 matrix model.

Again, the barrier inferred from where the σ^* and π^* diabatic curves intersect (21.5 kcal mol^{-1}) is not nearly as close to the ab initio barrier (17.6 kcal mol^{-1}) as is the result of our model (17.8 kcal mol^{-1}). Of course, the difference (21.5−17.8) of 4 kcal mol^{-1} is the value of $|V|$ for this case. Equally importantly, the model calculations required us to compute only one anion energy in a region where the anion is electronically metastable, which represents a substantial computational savings given the severe difficulty of performing stabilization calculations on such large species.

Finally, let us consider the case in which we expect the model to perform least satisfactorily because of the spatial proximity of the π^* and σ^* orbitals. In Figure 13, we show results for electron energies of 2 and 3 eV for the sugar−phosphate−sugar system described earlier (see Figures 8 and 9). For each energy, the model diabatic curves are shown on the left, and the results of the 2×2 matrix model appear on the right.

Clearly, the 2×2 matrix model is not able to reproduce the shape of the lower adiabatic anion curve in the small-R region (compare Figures 9 and 13) because the π^* anion curve in this case is not as well represented by the neutral's curve shifted upward by the electron's kinetic energy ($E = 2-3$ eV). This, in turn, is due to the fact that the P═O π bond is in close proximity to the phosphate−sugar O−C σ bond that cleaves. Nevertheless, the 2×2 model does a reasonably good job in the barrier regions of the potential surface even for this case in which we expect the model to perform least satisfactorily.

IV. Summary

In this report, we describe a computational model that allows us to avoid having to perform a very large number of tedious calculations on electronically metastable anions when studying indirect DEA processes. The model requires us to compute an adiabatic electronic state for the metastable anion at only a single geometry to extract a coupling parameter V. Specifically, the model involves the following steps:

(1) One computes the energy of the neutral molecule whose DEA is to be simulated as a function of the bond length (R) being considered for fragmentation.[19]

(2) One computes the energy of the anion at longer bond lengths, where the anion is electronically stable, and one extrapolates this repulsive energy curve to smaller R values. The resulting energy curve then represents one of the two diabatic anion states for this system.

(3) One approximates the second diabatic anion state by shifting the energy curve of the neutral molecule to higher energy by an amount equal to the energy E of the incident electron. This energy must lie within the Heisenberg width of this state; if the resonance energy of this state is not known from experiment or theory, it can be computed at the neutral's equilibrium geometry using stabilization-type methods.

(4) Using the above two diabatic curves as diagonal elements of a 2×2 Hamiltonian matrix, one computes, at a single R value,[17] the lowest adiabatic energy of the anion. This step requires the use of specialized techniques such as the stabilization method[13] to properly evaluate the energy of the metastable

anion. The energy obtained in this calculation can then be used to extract the off-diagonal element of the 2×2 Hamiltonian matrix.

(5) One then uses the two eigenvalues of the 2×2 matrix to approximate the lower and upper adiabatic anion energies at any R value. In particular, the lowest eigenvalue, computed over a range of R values, gives the adiabatic surface on which DEA flux will evolve once the incident electron attaches.

In this report, we have also demonstrated the value and accuracy of the proposed model. It is our intention to make substantial use of this approach when faced with having to compute the neutral and two diabatic anion energies (that latter often being metastable) in a wide range of future studies.

Acknowledgment. This work was supported by the NSF, Grants 9982420 and 0240387 to J. S., and by the Polish State Committee for Scientific Research (KBN), Grant DS/8371-4-0137-4 to P. S. Significant computer time provided by the Center for High Performance Computing at the University of Utah and by the Academic Computer Center in Gdansk (TASK) is also gratefully acknowledged.

References and Notes

(1) Dezarnaud-Dandine, C.; Bournel, F.; Troncy, M.; Jones, D.; Modelli, A. *J. Phys. B: At. Mol. Opt. Phys.* **1998**, *31*, L497−L502.

(2) Pearl, D. M.; Burrow, P. D.; Nash, J. J.; Morrison, H.; Nachtigallova, D.; Jordan, K. D. *J. Chem. Phys.* **1995**, *99*, 12379−12381. This paper contains a very nice discussion of how DEA yields can be used to probe the through-bond couplings that arise in such indirect DEA processes.

(3) There will be a range of energies around the nominal resonance energy because the π^* anion is metastable with respect to electron detachment. A typical lifetime for such a π^*-shape resonance is 10^{-13}−10^{-14} s, whereas that for a σ^*-shape resonance such as occurs in direct DEA processes is 10^{-14}−10^{-15} s. These rates correspond to Heisenberg widths of 0.04−4 eV. Of course, the electron attachment efficiencies for E values lying within the Heisenberg widths of the resonance energy will not be uniform.

(4) As noted in ref 3, both the σ^* and π^* anion states have significant Heisenberg uncertainties in their energies. In this paper, when we refer to an energy curve of one of these states we mean the central energy of that resonance state as a function of bond length. When we speak of the electron's kinetic energy that generates one of these states, we mean that the electron has an energy E lying within the Heisenberg width of that state we claim to be generated by electron capture.

(5) Barrios, R.; Skurski, P.; Simons, J. *J. Phys. Chem. B* **2002**, *106*, 7991−7994.

(6) Berdys, J.; Anusiewicz, I.; Skurski, P.; Simons, J. *J. Phys. Chem.* **2004**, *A108*, 2999−3005.

(7) Berdys, J.; Anusiewicz, I.; Skurski, P.; Simons, J. *J. Am Chem. Soc.* **2004**, *126*, 6441−6447.

(8) Berdys, J.; Skurski, P.; Simons, J. *J. Phys. Chem. B* **2004**, *108*, 5800−5805.

(9) Anusiewicz, I.; Berdys, J.; Sobczyk, M.; Skurski, P.; Simons, J. *J. Phys. Chem. A* **2004**, *108*, 11381−11387.

(10) Miertus, S.; Tomasi, J. *Chem. Phys.* **1982**, *65*, 239−242. Cossi, M.; Barone, V.; Cammi, R.; Tomasi, J. *Chem. Phys. Lett.* **1996**, *255*, 327−335.

(11) Of course, at even larger R values, a minimum can develop in these curves because of the long-range charge−dipole and charge−induced-dipole interactions.

(12) Even if one uses nonvariational methods such as Møller−Plesset perturbation theory (MPn) or coupled-cluster theory (CC) to compute the neutral and anion energies, an initial step in such calculations involves performing a Hartree−Fock self-consistent field (SCF) calculation to obtain appropriate orthonormal molecular orbitals. Because SCF calculations are variational, it is at this step that the collapse most likely occurs.

(13) Hazi, A. U.; Taylor, H. S. *Phys. Rev. A1* **1970**, 1109. Simons, J. *J. Chem. Phys.* **1981**, *75*, 2465; Frey, R. F.; Simons, J. *J. Chem. Phys.* **1986**, *84*, 4462.

(14) For example, to evaluate the energy of a metastable state at one value of R, we need to carry out a series of calculations (typically 4−10) in which we have added a stabilizing potential of varying strength to the anion's molecular framework. By then extrapolating our findings to zero strength of this stabilizing potential, we achieve our estimate of the metastable state's energy. Each of these 4−10 calculations is at least as computationally demanding as calculating the energy of the corresponding neutral or its anion at R values where the anion is electronically bound.

(15) We fit the σ^* energy data to the functional form $C + A \exp[-b(R - R_c)]$, where R_c is the value of R at which the σ^* energy intersects the neutral's energy curve and A, C, and b are parameters whose values we obtained by least-squares fitting. It turns out that the functions thus obtained represent very well the σ^* anion's energy at shorter R values where this state is electronically metastable. We verified this by performing the time-consuming stabilization calculations on these σ^* states at several R values to test the quality of the above exponential functional form.

(16) We realize that this coupling is most likely R-dependent. However, to form a model that contains the fewest parameters, we assume that this matrix element is a constant. Of course, the ultimate judge for this assumption will be to see how well this model works.

(17) Actually, we can carry out such a calculation at any R value. Knowing E_-, E_{σ^*}, and E_{π^*} at any R, we can use the quadratic equation to determine $|V|$. However, we choose to compute $|V|$ by using a value of E_- near the crossing of E_{σ^*}, and E_{π^*} because it is in this region that the coupling is most important; we feel that we achieve optimal numerical significance by computing $|V| = E_{\sigma^*} - E_-$ at such an R value.

(18) We could have evaluated the upper adiabatic surface's energy and used it in the quadratic equation to determine $|V|$, but the lower adiabatic energy is almost always computationally easier to determine.

(19) In such a calculation, all other geometrical degrees of freedom are relaxed to minimize the energy. Of course, in doing such a relaxation, one can also notice which geometrical degrees of freedom are changed most.